

Functionalized SBA-15 by amine group for removal of Ni(II) heavy metal ion in the batch adsorption system

Talib M. Albayati*, Anaam A. Sabri, Dalia B. Abed

Department of Chemical Engineering, University of Technology, 52 Alsinaa St., P.O. Box: 35010, Baghdad, Iraq, emails: 80046@uotechnology.edu.iq (T.M. Albayati), aaksabri@yahoo.com (A.A. Sabri), dalea595@yahoo.com (D.B. Abed)

Received 7 May 2019; Accepted 28 August 2019

ABSTRACT

In this work, several variables that can affect the adsorption of Ni(II) using NH₂-SBA-15 were studied in a batch adsorption system including; pH (1–6), contact time (0–150 min), initial concentration (20–120 mg L⁻¹), NH₂-SBA-15 dose (0.025–0.3 g) and temperature (293–333 K). The removal percentage increased with increasing the pH, the contact time, NH₂-SBA-15 dose and temperature, while the increase of the initial concentrations for this metal ion reduced their percentage removal. It appeared that the Langmuir adsorption isotherm model had the best fit with $R^2 = 0.99$, and the maximum capacity of monolayer adsorption increased from 64.52 to 90.1 mg g⁻¹ as increasing in the temperature from 293 to 333 K, respectively. It was demonstrated that the kinetic studies were fitted well with the pseudo-second-order kinetic model ($R^2 = 0.99$). The results of thermodynamic parameters showed that the process is endothermic chemisorption ($\Delta H^\circ = 93.8734$ kJ mol⁻¹) with a very little degree of disorder ($\Delta S^\circ = 0.38812$ kJ mol⁻¹ K⁻¹) and whenever the temperature increased from 293 to 333 K, the process became more spontaneous ($\Delta G^\circ = -19.098$ to -34.33 kJ mol⁻¹ K⁻¹).

Keywords: Heavy metal; Ni(II) Removal; Adsorption; Batch adsorption; Wastewater treatment; Functionalization; Nanoporous SBA-15.

1. Introduction

Heavy metals are non-biodegradable, toxic and carcinogenic even at low concentrations, and they can be cumulative in living tissues, causing different diseases and disturbances [1]. As a result, environmental regulations and legislation for wastewater discharge have been issued by government agencies and international organizations, such as the Environmental Protection Agency and World Health Organization [2].

Due to their toxicity to higher life forms and mobility in natural water ecosystems, heavy metal ions in ground supplies and wastewater have been considered as major inorganic contaminants in the water pollution and environment; therefore, they must be removed before discharged [3].

Traditional treatment methods include; chemical oxidation, reduction or chemical precipitation, ion exchange, filtration, electrochemical treatment, evaporation recovery and membrane technologies [4]. However, some of these methods can be extremely expensive or ineffective at very low concentrations (1–100 mg L⁻¹). Another important disadvantage resulted from applying some of these processes is the generation of toxic chemical sludge. Therefore, the reduction of toxic heavy metals in an environment-friendly approach, such as adsorption, is not only highly efficient but also cost-effective [5]. It is also well known for its relatively low effectiveness and that it doesn't acquire high technical expertise, in addition to the fact that it offers promising removal efficiencies even with dilute solutions [6,7]. More recently, researchers developed adsorbents, which are

* Corresponding author.

cheap, easily available and do not need special maintenance during operational conditions [8,9]. For example; Bhatti et al. [10] investigated the phosphate ions removal in aqueous medium mango stone biocomposite efficiency for the removal of phosphate ions (PO_4^{3-}) from aqueous solution. Kausar et al. [11] evaluated the removal of strontium ion from aqueous solutions using peanut husk, an agricultural waste, as a new adsorbent. A wide variety of adsorbents, such as zeolites, activated carbon, clays, and agricultural residues have been used for the removal of heavy metal ions [12]. However, the essential problem in this field is to choose novel kinds of adsorbents that meet specific requirements, including geometry with an open pore structure and well-designed pore size [13]. Nanoporous materials, as a subset of nanostructured materials, have been the center of interest for many researchers throughout the world. They are divided into three types (depending on their pore sizes which range from 1 to 100 nm): microporous, mesoporous and macroporous materials [14]. Since its discovery in 1998 by Zhao et al. [15,16] SBA-15 has attracted great interest as a potential adsorbent, catalyst support, drug delivery, and hydrogen storage. Amino-functionalized mesoporous silica has been used for different applications other than adsorption, including protein sequestration and release, enzyme immobilization, drug delivery, mainly due to its high stability and relatively simple synthesis [17]. In the present work, amino-functionalized mesoporous silica NH_2 -SBA-15 is used as an effective adsorbent for the adsorption of Ni(II) heavy metal ions from simulated wastewater. So, the major aim of the present study was to determine the ability of amine-functionalized SBA-15 as an adsorbent to remove Ni(II) heavy metal ion from wastewater in a batch adsorption system.

2. Materials and methods

2.1. Chemicals

Pluronic "P123" tetraethyl orthosilicate (TEOS, 98%), hydrochloric acid (HCl), distilled water (H_2O), toluene ($\text{C}_6\text{H}_5\text{-CH}_3$), (3-aminopropyl)triethoxysilane (APTES), ($\text{H}_2\text{N}(\text{CH}_2)_3\text{Si}(\text{OC}_2\text{H}_5)_2$, 99%), nickel (II) nitrate hexahydrate ($\text{Ni}(\text{NO}_3)_2 \cdot 6\text{H}_2\text{O}$, 99%) and Sodium hydroxide (NaOH, 99%). All chemicals were applied as acquired without additional purification.

2.2. Synthesis of SBA-15 and characterization

The synthesis of pure mesoporous SBA-15 and functionalized NH_2 -SBA-15 as a nanoporous adsorbent for Ni(II) ion in batch adsorption system was achieved according to the traditional method [18,19]. The characterizations were carried out on the pure SBA-15 and NH_2 -SBA-15 in our previous study as well [20–22].

2.3. Preparation of metal solution

The stock solutions ($1,000 \text{ mg L}^{-1}$) of Ni(II) metal was prepared by dissolving a predetermined amount of metal salt $\text{Ni}(\text{NO}_3)_2 \cdot 6\text{H}_2\text{O}$ in distilled water. Then the required concentration of the metal solution was prepared by dilution with distilled water. The concentrations of metals ions before and

after removal were measured by using the atomic absorption spectrophotometer (SHIMADZU AA-7000, Japan).

2.4. Batch adsorption

The equilibrium experiments were done by agitating of known amounts of NH_2 -SBA-15 with 100 ml of metal solutions in different concentrations of known pH (adjusted by using 0.1 N of HCl or NaOH) with 240 rpm at room temperature. While kinetic experiments were performed at different temperatures by taking 1 L flask containing a 1 L metal solution of known pH and concentration, after adsorbent addition the mixture was stirred by a magnetic stirrer at 240 rpm. After a certain time, the adsorbent was separated by filtration using filter paper (Whatman 542, England) and then the samples were analyzed by atomic absorption spectrophotometer for metals analysis. The range of parameters that were studied as follows: pH 1–6, contact time 0–150 min, NH_2 -SBA-15 dose 0.025–0.3 g, the initial concentration of metal ions ($20\text{--}120 \text{ mg L}^{-1}$) and Temperature $20^\circ\text{C}\text{--}60^\circ\text{C}$.

The uptake of heavy metal ion was calculated from the following equation:

$$q_e = \frac{V(C_0 - C_e)}{W} \quad (1)$$

where q_e is equilibrium adsorption capacity of the adsorbent, C_0 and C_e are initial and equilibrium concentration respectively in (mg L^{-1}), V is the volume of solution in (L) and W is the weight of the adsorbent in (g). The uptake of metal ions at any time was calculated from Eq. (2).

$$q_t = \frac{V(C_0 - C_t)}{W} \quad (2)$$

where q_t and C_t are the adsorption capacity in (mg g^{-1}) and metal ion concentration in solution in (mg L^{-1}) respectively at time t . The removal efficiency was calculated by the following equation:

$$\%R = \frac{C_0 - C_e}{C_0} \times 100\% \quad (3)$$

2.5. Adsorption isotherms models

2.5.1. Langmuir isotherm model

The adsorption model proposed by Langmuir is based on monolayer adsorption, where adsorption can exclusively take place at definite sites that are fixed in number, equivalent, and identical.

The Langmuir equilibrium adsorption equation has the form [23].

$$q_e = \frac{q_{\max} b C_e}{1 + b C_e} \quad (4)$$

where q_e is equilibrium adsorption capacity of the adsorbent in (mg g^{-1}) q_{\max} is the maximum adsorption capacity in (mg g^{-1}), C_e is the equilibrium concentration in (mg L^{-1}), and

b is the Langmuir constant in (L mg⁻¹) which represents the degree of adsorption affinity of the adsorbate. The higher the value of b , the stronger is the affinity of the ion towards adsorbent. Eq. (4) can be used as a linear form as follows:

$$\frac{C_e}{q_e} = \frac{1}{q_{\max}} C_e + \frac{1}{bq_{\max}} \quad (5)$$

R_L is a dimensionless constant which is known as separation factor or equilibrium parameter and represented as [24]

$$R_L = \frac{1}{1 + bC_0} \quad (6)$$

This parameter shows the isotherm is favorable ($R_L < 1$), unfavorable ($R_L > 1$), irreversible ($R_L = 0$), or linear ($R_L = 1$) [25]

2.5.2. Freundlich isotherm model

Freundlich model is the first expression to describe multilayer adsorption. The Freundlich isotherm is an empirical equation employed to describe heterogeneous systems, it is expressed as:

$$q_e = K_f C_e^{1/n} \quad n > 1 \quad (7)$$

The linearized Freundlich isotherm equation can be expressed as:

$$\ln q_e = \ln K_f + \frac{1}{n} \ln C_e \quad (8)$$

where n and K_f are the constants of Freundlich related to intensity and capacity of adsorption, respectively. from the slope and intercept of the linear plot for experimental data $\ln q_e$ vs. $\ln C_e$, the values of n and K_f can be calculated where $(1/n)$ is the slope and $\ln K_f$ is the intercept. The slope with a range between zero and unity and is an indication of heterogeneity of the surface and the intensity of adsorption, as the slope is very low (near zero). Whereas a slope near unity refers to a chemisorption process, where $1/n$ higher than unity implies cooperative adsorption [26].

2.5.3. Temkin isotherm model

This model assumes a uniform distribution of surface binding energy, and that for all the molecules, the adsorption heat decreases linearly upon an increase in the adsorbent surface coverage, this model is expressed as follows [27].

$$q_e = \frac{RT}{b_T} \ln A_T C_e \quad (9)$$

where A_T is the binding constant of equilibrium (L g⁻¹) identical to the extreme binding energy, b_T is Temkin isotherm constant and is regarding to adsorption heat (J mol⁻¹), R is the universal gas constant (8.314 J mol⁻¹ K⁻¹), and T is absolute temperature (K). Eq. (9) can be written in the linear form as follows:

$$q_e = \frac{RT}{b_T} \ln A_T + \frac{RT}{b_T} \ln C_e \quad (10)$$

A_T and b_T is the isotherm constants which can be evaluated from the plot of q_e vs. $\ln C_e$.

2.6. Adsorption kinetics

2.6.1. Pseudo-first-order model

Pseudo-first-order kinetic equation can be written as follows [28].

$$\frac{dq_t}{dt} = k_{p1} (q_e - q_t) \quad (11)$$

where q_t and q_e are the amounts adsorbed (mg g⁻¹) at time t and equilibrium, respectively. Integration and rearrangement of Eq. (11) give:

$$\ln(q_e - q_t) = \ln q_e - k_{p1} t \quad (12)$$

where k_{p1} is rate constant of the pseudo-first-order for adsorption (h⁻¹) and from the slope of the linear plot of $\ln(q_e - q_t)$ vs. t which can be calculated.

2.6.2. Pseudo-second-order model

The pseudo-second-order kinetic equation is given as [29].

$$\frac{dq_t}{dt} = k_{p2} (q_e - q_t)^2 \quad (13)$$

The differential equation is usually integrated and transformed into its linear form:

$$\frac{t}{q_t} = \frac{1}{k_{p2} q_e^2} + \frac{1}{q_e} t \quad (14)$$

where k_{p2} is the pseudo-second-order rate constant for adsorption (g mg⁻¹ min⁻¹) and can be determined by plotting t/q_t vs. t .

2.6.3. Intraparticle diffusion model

Transportation of the adsorbate from the bulk liquid to the adsorbent surface occurs in multiple stages. Those stages may affect the overall adsorption process including external mass transfer, intraparticle mass transfer, and pore surface adsorption. The intraparticle diffusion model is applied to investigate the possibility of the intraparticle mass transfer. This model is expressed as in the following equation [30].

$$q_t = k_{id} t^{0.5} + C \quad (15)$$

where k_{id} is the rate constant for intraparticle diffusion (mg g⁻¹ min^{-0.5}), C is the intraparticle diffusion constant. If a straight line resulted from plotting q_t vs. $t^{0.5}$, then the overall process of adsorption is exclusively limited intraparticle

mass transfer. However, if more than one linear plot resulted from plotting the data, then more than one stage of the previously mentioned stages has a strong effect on the overall process of adsorption [31]. The values of C is an indication of boundary layer thickness, the smaller the intercept, the weaker the effect of the boundary layer [32].

2.7. Adsorption thermodynamics

The ability of adsorption can be greatly affected by temperature. Temperature changes can cause changes in thermodynamics and kinetic energy. Spontaneity and feasibility of the process can be obtained from thermodynamic data such as Gibbs free energy (ΔG°), enthalpy (ΔH°), and entropy (ΔS°) which are all temperature-dependent. The system's kinetic energy is also influenced by temperature changes because molecules' diffusion rate is a function of temperature. Generally, a faster adsorption rate can be achieved by elevating the temperatures [33].

The thermodynamic parameters were determined from the classical linear form of Van't Hoff equation Eq. (16).

$$\ln K_d = -\frac{\Delta H^\circ}{RT} + \frac{\Delta S^\circ}{R} \quad (16)$$

where ΔH° (change in enthalpy (J mol^{-1})) and ΔS° (change in entropy ($\text{J mol}^{-1} \text{K}^{-1}$)) values obtained from the slope and intercept of $\ln K_d$ vs. $1/T$ plots. T is the temperature in K, R is the universal gas constant ($8.314 \text{ J mol}^{-1} \text{K}^{-1}$) and K_d is the distribution coefficient which was determined from the following equation [34].

$$K_d = \frac{q_e}{C_e} \quad (17)$$

The Gibbs free energy is calculated according to the following equation:

$$\Delta G^\circ = -RT \ln K_d \quad (18)$$

where ΔG° is standard free energy change (J mol^{-1}) [35].

3. Results and discussions

3.1. Batch adsorption

3.1.1. Effect of pH

The pH of the solution is one of the most remarkable parameters controlling the sorption process. The experimental results reveal that Ni(II) ion adsorption using NH_2 -SBA-15 was best at a pH range of 1–6. The obtained results are shown in Fig. 1. It can be noted that as the pH increased, the adsorption efficiency increased as well. These results can be explained in terms of the protonation of the amino groups, at lower pH values, leading to a positively charged surface. Repulsive forces between the positively charged Ni(II) ion and the positively charged surface reduce the overall adsorption efficiency. Moreover, as the pH of the solution increases (up to 5) the repulsion between the surface and metals cations decreases due to the decreasing in

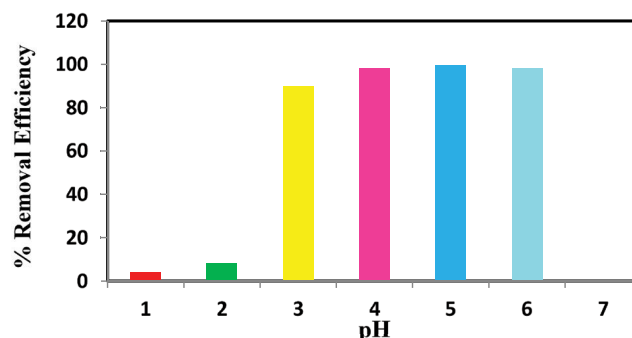


Fig. 1. Effect of pH on the removal efficiency of Ni(II) ion ($C_0 = 100 \text{ mg L}^{-1}$, contact time = 60 min, NH_2 -SBA-15 dosage = 0.1 g, and at room temperature).

amine group protonation, and subsequently, the increase in the extent of formation of a complex between metal ion and the amine groups led to increasing the removal efficiency of Ni(II) up to 99.27%. When the pH increased more than 5 (at pH 6) a slight decrease in removal efficiency 98.7% was observed, this is due to the precipitation of the metal ions as its hydroxides would be formed. Therefore, neither precipitation of the metal hydroxide nor protonation of the amine groups occurs at the best value of pH is 5 for Ni(II) removal from aqueous solution [36].

3.1.2. Effect of contact time

The relationship between contact time and the percentage removal of Ni(II) by NH_2 -SBA-15 at room temperature is shown in Fig. 2. the removal efficiency increases with time until equilibrium adsorption is established. In the first 15 min, there is a rapid increase in the removal efficiency; this is due to the existence of a great number of unoccupied surface sites for adsorption at the start. It was also suggested that the high sorption rate with increasing time be due to the attraction of active functional groups (NH_2) toward metals ions which led to the stronger surface binding. With the progress in contact time, the surface adsorption sites become exhausted and no significant increase in removal efficiency will occur, and then the equilibrium will be established. The highest removal efficiency was 99%, after 60 min [37].

3.1.3. Effect of initial concentration

The effects of initial Ni(II) concentration on adsorption behavior were investigated as shown in Fig. 3 This figure reveals the removal efficiency decreases as the initial heavy metal concentration increases. This can be simply attributed to the saturation of the limited number of adsorbents active sites up to a certain Ni(II) concentration. There is a slight drop in the percentage removal of Ni(II) at a higher initial concentration.

3.1.4. Effect of NH_2 -SBA-15 dose

The effect of NH_2 -SBA-15 dose was studied and the results are shown in Fig. 4. The results assure that as NH_2 -SBA-15 dose increased, the removal efficiency of Ni(II) also

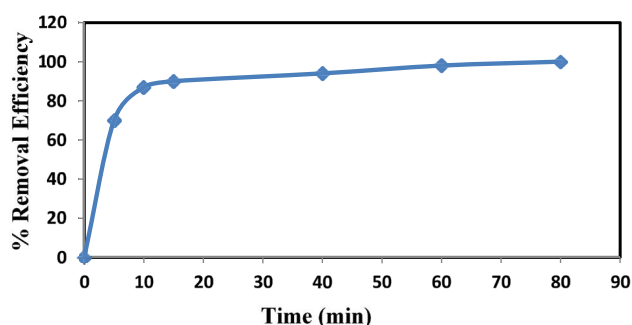


Fig. 2. Effect of contact time on the removal efficiency of Ni(II) ions ($C_0 = 100 \text{ mg L}^{-1}$, $\text{pH} = 5$, $\text{NH}_2\text{-SBA-15}$ dose = 1 g, and volume = 1 L).

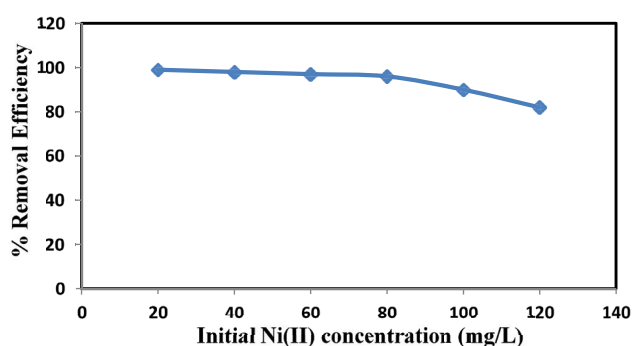


Fig. 3. Effect of initial metal concentration on the removal efficiency of Ni(II) ($\text{pH} = 5$, time = 90 min, $\text{NH}_2\text{-SBA-15}$ dose = 0.1, volume = 100 ml, and at room temperature).

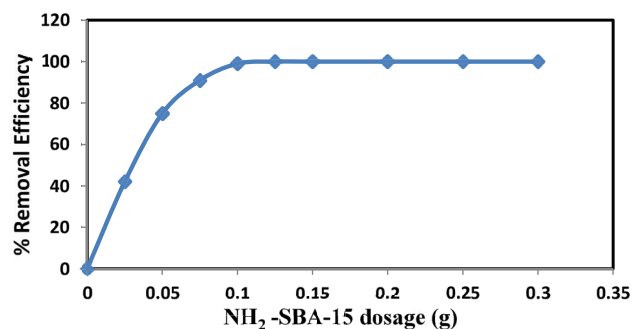


Fig. 4. Effect of $\text{NH}_2\text{-SBA-15}$ dose on Ni(II) removal, ($C_0 = 100 \text{ mg L}^{-1}$, $\text{pH} = 5$, time = 60 min, volume = 100 ml, and at room temperature).

increased, up until 0.1 g of $\text{NH}_2\text{-SBA-15}$, achieving the highest removal efficiency. The increase in removal efficiency is attributed to that the highest dosage of adsorbent in the solution means the available higher total surface area and more active sites for the metals ion binding, consequently decreasing the number of ions remaining in the solution [38].

3.1.5. Effect of temperature

The effect of temperature on Ni(II) adsorption by $\text{NH}_2\text{-SBA-15}$ was studied at 293, 313, and 333 K with different

initial concentrations 20–100 mg L^{-1} . Fig. 5 clearly shows the significant effect of temperature on Ni(II) adsorption. At a constant initial Ni(II) concentration, as temperature increased from 293 to 333 K, the removal efficiency also increased. For instance, at 60 mg L^{-1} Ni(II) initial concentration, the removal efficiency increased from 85.7% to 99.3%. It can also be observed that as the initial concentration increased, the temperature effect on removal efficiency also intensified. The kinetic energy of metal ions in solution increases because of the increases in temperature and in which the number of metal ions reaching the adsorbent surface increased [34].

3.2. Adsorption isotherms

The adsorption isotherm was conducted at equilibrium conditions on the removal of Ni(II) ion from an aqueous solution to obtain a relationship between the quantity of Ni(II) ions adsorbed onto the SBA-15 and that retained in the aqueous solution. Experimental data obtained from the study were fitted to three different isotherm models.

The experimental data were fitted to three linearized isotherm models (Langmuir, Freundlich, and Temkin) at three temperatures (293, 313, and 333 K). For these models, the obtained parameters and the regression correlation coefficient (R^2) are listed in Table 1. It is clear from Table 1 that the Langmuir isotherm model has the best fitting for the sorption of Ni(II) on $\text{NH}_2\text{-SBA-15}$ at various temperatures ($R^2 \sim 0.99$). Therefore, the adsorption process can be described by the formation of monolayer coverage of the adsorbate on the homogeneous adsorbent surface. The calculated maximum adsorption capacity (q_{max}) Eq. (5) of $\text{NH}_2\text{-SBA-15}$ was found to be closer to the experimental value (89.5 mg g^{-1}), also it increases from 64.52 to 90.1 mg g^{-1} as the temperature of the solution increased from 293 to 333 K. Higher temperature enhances both chemisorptions (as it is a chemical reaction), and physisorption (as it facilitates the passing of Ni(II) from the external surface throughout the enlarged pores) [39]. The comparison of q_{max} result for Ni(II) removal by $\text{NH}_2\text{-SBA-15}$ with some other studies is higher than from some examples, $q_{\text{max}} = 81.812 \text{ mg g}^{-1}$ and $q_{\text{max}} = 22 \text{ mg g}^{-1}$, as obtained by [40,41]. The equilibrium parameter or dimensionless separation factor R_L based on the Langmuir equation was used to predict the favorability of the adsorption system, Table 1. shows the R_L values based on the Langmuir

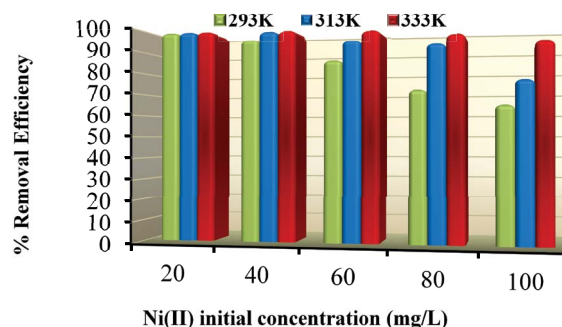


Fig. 5. Effect of temperature on Ni(II) percentage removal with different initial concentration (time = 90 min, $\text{NH}_2\text{-SBA-15}$ dose = 0.1 g, volume = 100 ml and $\text{pH} = 5$).

Table 1
Model parameters for Ni(II) adsorption on NH₂-SBA-15

Isotherm model	293 K	313 K	333 K
Langmuir:			
q_{max} (mg g ⁻¹)	64.52	76.92	90.1
b (L mg ⁻¹)	0.799	3.095	6.166
R^2	0.9931	0.9983	0.9991
R_L	0.0123	3.2×10^{-3}	1.62×10^{-3}
Freundlich:			
K_f (mg ¹⁻ⁿ g ⁻¹ L ⁿ)	34.046	49.264	62.33
$1/n$	0.1722	0.1698	0.2151
R^2	0.9924	0.8749	0.8942
Temkin:			
b_t (J mol ⁻¹)	368.45	346.78	263.5
A_t (L g ⁻¹)	313.69	1430.8	620
R^2	0.9834	0.9319	0.9842

isotherm model, in which all R_L values are greater than 0 but less than 1 indicating that Langmuir isotherm is favorable.

3.3. Adsorption kinetics

To study adsorption kinetics; pseudo-first-order, pseudo-second-order, and intraparticle diffusion models are applied. Contact time from experimental results can be used to study the rate-limiting step in the adsorption mechanism in a given system.

3.3.1. Effect of temperature

At a constant initial Ni(II) concentration of 80 mg L⁻¹, the effect of temperature change on adsorption kinetics was studied at 293, 313 and 333 K as shown in Fig. 6. It can be noticed that the adsorbed quantity of Ni(II) ions has increased as the temperature increased, which leads to the conclusion that the overall process is endothermic. Several amine groups hydrogen-bonded to the hydroxyl groups of silica surface causes the enhancement of Ni(II) ions uptake with increasing temperature and its availability for adsorption is decreasing. The highest capacity of adsorption was achieved by increasing temperature supply's enough energy which breaks these bonds and releases the amine groups.

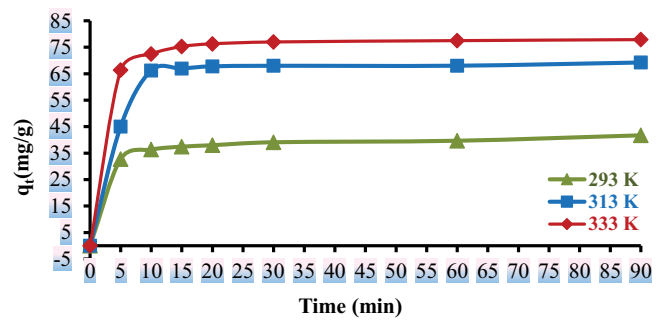


Fig. 6. Effect of temperature on the uptake of Ni(II) at NH₂-SBA-15 versus time ($C_0 = 80$ mg L⁻¹, pH = 5, volume = 1 L, NH₂-SBA-15 dose = 1 g).

Table 2 shows the parameters related to Pseudo-first-order and second-order kinetic models, along with the resulted correlation coefficients (R^2). It can be observed that pseudo-second-order has better fitted the experimental data, based on correlation coefficients (R^2) result and the proximity between the both experimental and predicted (q_e), compared to those resulting from the first-order kinetic model [42].

3.3.2. Effect of initial concentration

Fig. 7 presents the effect of three different Ni(II) initial concentrations, 40, 60 and 80 mg L⁻¹ on adsorption kinetics, was investigated at 333 K. The uptake rate was somewhat fast during the initial stage of adsorption. That could be inclined to the presence of readily available adsorption sites in addition to the initial high adsorption gradient. The uptake rate then slows down gradually until equilibrium is established.

From the linear fits of the pseudo-second-order model, it acquires the regression coefficients (R^2) a good correlation for the three initial concentrations. Table 2 also shows that the pseudo-second-order constants decrease from 0.0539 to 0.0238 g mg⁻¹ min⁻¹ when the initial nickel concentration increased from 40 to 80 mg L⁻¹, respectively [43].

3.4. Prediction of Ni(II) adsorption kinetics

The values of q_e resulted by applying both temperatures and initial concentrations in a predetermined range are shown in Fig. 8, the following relationships were obtained:

$$q_e = 0.9114T - 222.34 \quad (19)$$

Table 2
Effect of solution temperature and initial concentration on Ni(II) adsorption kinetics

Pseudo-first-order model				Pseudo-second-order model				
Temperature (K)	C_0 (mg L ⁻¹)	$q_{e,exp}$ (mg g ⁻¹)	R^2	k_{p1} (min ⁻¹)	$q_{e,mod}$ (mg g ⁻¹)	R^2	k_{p2} (g min ⁻¹ mg ⁻¹)	$q_{e,mod}$ (mg g ⁻¹)
293	80	41.7227	0.5843	0.038	11.989	0.9989	0.0164	41.67
313	80	69.231	0.506	0.0545	12.16	0.9999	0.02	68.966
333	80	77.883	0.7467	0.0756	16.029	0.9999	0.0238	78.125
333	60	59.17	0.9715	0.0609	48.46	0.9999	0.029	59.524
333	40	39.9848	0.5843	0.038	11.989	0.9999	0.0539	40.16

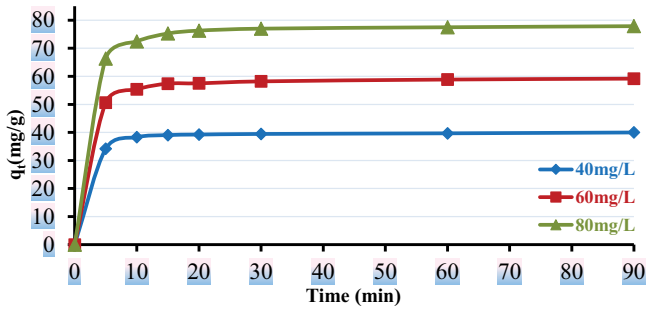


Fig. 7. Kinetics of Ni(II) adsorption on NH₂-SBA-15 at different initial concentrations (pH = 5, volume = 1 L, NH₂-SBA-15 dose = 1 g, and at temperature = 333 K).

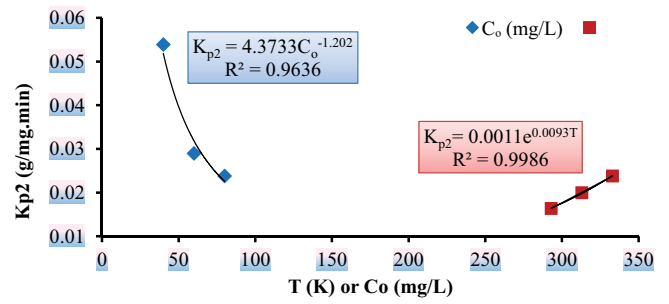


Fig. 9. Relationships of pseudo-second-order constants with and initial concentration.

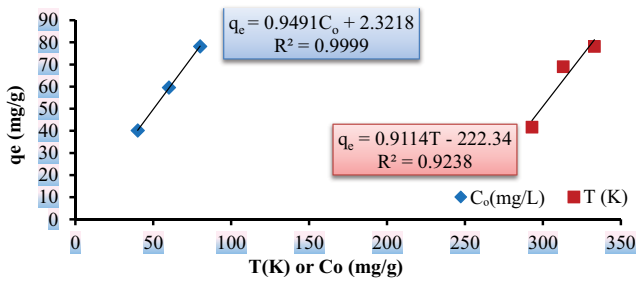


Fig. 8. Relationships of equilibrium capacities with temperature and initial concentration.

$$q_e = 0.9491C_0 + 2.3218 \quad (20)$$

The relationships between pseudo-second-order constants with temperature and initial concentration are shown in Fig. 9 and described by the following equations:

$$K_{p2} = 0.0011e^{0.0093T} \quad (21)$$

$$K_{p2} = 4.3733C_0^{-1.202} \quad (22)$$

The relationships of Eqs. (19)–(22) manipulate in a model of pseudo-second-order to obtain predicted as a general model for the relationships between the adsorption uptake q (mg g⁻¹) along with solution temperature (K) Eq. (23) and initial concentration (mg L⁻¹) Eq. (24) at any time (min) that can be described as:

$$q_{(T)} = \frac{0.0011e^{0.0093T} (0.9114T - 222.34)^2 t}{1 + 0.0011e^{0.0093T} (0.9114T - 222.34)t} \quad (23)$$

$$q_{(C_0)} = \frac{4.3733C_0^{-1.202} (0.9491C_0 + 2.3218)^2 t}{1 + 4.3733C_0^{-1.202} (0.9491C_0 + 2.3218)t} \quad (24)$$

Both general models were applied to the initial concentrations and three different temperatures and the outcomes are shown in Figs. 10 and 11, which show a good agreement between the experimental data and the data predicted from the general models for both situations.

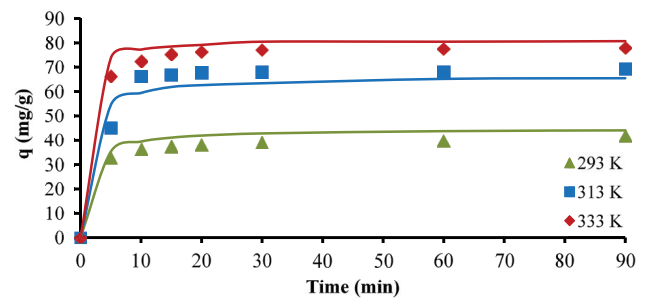


Fig. 10. Validity of the generalized predictive model for different temperatures (solid lines: model, symbols: experimental data).

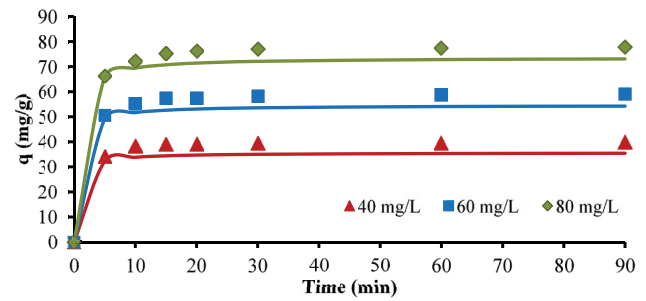


Fig. 11. Validity of the generalized predictive model for different initial nickel concentration (solid lines: model, symbols: experimental data).

3.5. Intraparticle diffusion model

The intraparticle diffusion model Eq. (15) was applied to the experimental data to show both the dominant mechanisms and the rate-controlling steps in Ni(II) adsorption process, as shown in Figs. 12 and 13. Both of the previously mentioned figures exhibit multi-linear plots represented by three stages, as specified by the dotted line, representing the rate change in the adsorbed nickel. The first stage represents a rapid increase in adsorption rate, this is due to the obtainability of free adsorption sites at the exterior surface of NH₂-SBA-15 and the concentration gradient of nickel ions. The external diffusion, which greatly affects the adsorption process, occurs. As illustrated in Figs. 12 and 13 the larger slope of these dotted lines in this region means a higher concentration gradient. After this stage and as time passed,

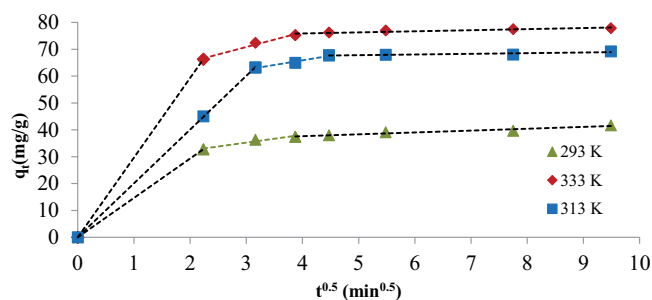


Fig. 12. Intraparticle diffusion of nickel adsorption onto $\text{NH}_2\text{-SBA-15}$ at different temperatures (pH = 5, dose = 1 g, volume = 1 L, $C_0 = 80 \text{ mg L}^{-1}$).

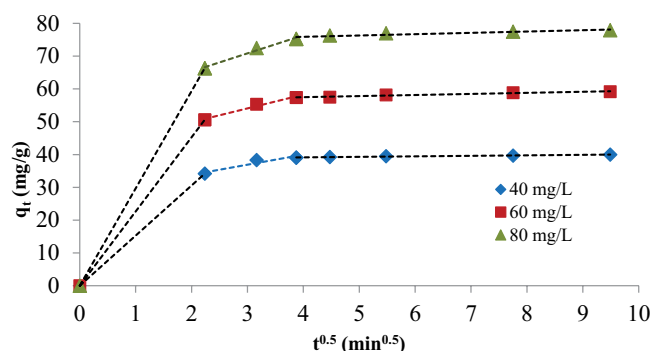


Fig. 13. Intraparticle diffusion of nickel adsorption onto $\text{NH}_2\text{-SBA-15}$ at different initial concentrations (pH = 5, dose = 1 g, volume = 1 L, $T = 333 \text{ K}$).

a quantity of nickel adsorbed decreased significantly, this is due to the saturation of the external sites of $\text{NH}_2\text{-SBA-15}$ and the decrease in a nickel concentration gradient. In this region, nickel ions will transport from bulk of solution to adsorbent external surface and then diffusion within pores will occur, this ultimately slows the adsorption process, compared to the first stage. Since the second portion of the plots in both figures did not have zero intercepts, so the intraparticle diffusion is not the only rate that controls the adsorption process. The values of k_{id} that are acquired from this step are calculated from the slope of the second stage line and the results are shown in Table 3.

Table 3 shows that k_{id} values increase from 2.8938 to 3.4587 and 5.5128 $\text{mg g}^{-1} \text{min}^{-0.5}$ with an increase in solution temperature from 293 to 313, and then 333 K respectively as a result of increasing the kinetic energy. The same effect was noticed in initial concentration, where the k_{id} increased

Table 3

Intraparticle diffusion model parameters at different temperatures and initial concentrations

Temperature (K)	C_0 (mg L^{-1})	k_{id} ($\text{mg g}^{-1} \text{min}^{-0.5}$)	R^2
333	80	5.5128	0.9818
313	80	3.4587	0.9656
293	80	2.8938	0.9537
333	60	4.1971	0.9773
333	40	3.0616	0.9082

from 3.0616 to 4.1971 and 5.5128 $\text{mg g}^{-1} \text{min}^{-0.5}$ as increasing in the initial concentration from 40 to 60 and then 80 mg L^{-1} respectively, this is mainly due to an increase in driving force because of an increase in the gradient of concentration. The horizontal dotted lines of Figs. 12 and 13 plots represent the third region in which very slower uptake of Ni(II) ions occurs; this is due to equilibrium adsorption [22].

3.6. Adsorption thermodynamics

The influence of temperature on Ni(II) ion adsorption using $\text{NH}_2\text{-SBA-15}$ is represented by the linear Van't Hoff plot ($\ln K_d$ vs. $1/T$) in Fig. 14. The slope and intercept of linear Van't Hoff plot Eq. (16) are used to determine ΔH° and ΔS° and then ΔG° from Eq. (18). The thermodynamic parameters ΔH° , ΔS° , and ΔG° are listed in Table 4. The positive value of ΔH° (93.8734 kJ mol^{-1}) indicates that the overall adsorption process is endothermic. This is appropriate with the increase in Ni(II) removal percentage temperature as shown in Fig. 5. Also, the ΔH° value is located within the range of 40–400 kJ mol^{-1} , which is the chemisorption range. The degree of the spontaneity of the adsorption process is determined using the values of Gibbs free energy and the decrease in ΔG° values with temperature increase from 293 to 333 K indicates a more spontaneity of nickel adsorption at highest temperatures. The entropic with a positive value indicates that the system has a disorder degree which was acquired during the adsorption process [44].

3.7. Comparison of present results with previous ones

The comparison between the functionalized SBA-15 with other adsorbents reported in the literature is shown in Table 5. This table is providing useful information about how efficient SBA-15- NH_2 adsorbent can enhance the

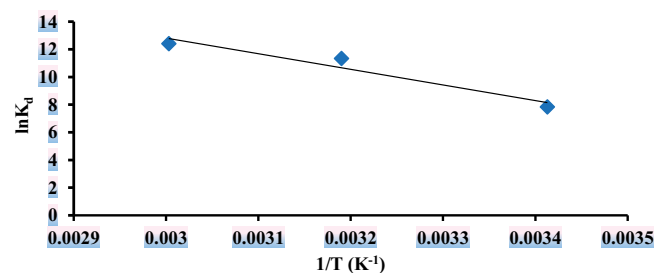


Fig. 14. Van't Hoff plot for Ni(II) adsorption on $\text{NH}_2\text{-SBA-15}$ ($C_0 = 80 \text{ mg L}^{-1}$, pH = 5, volume = 100 ml, dose = 0.1 g, time = 90 min).

Table 4

Thermodynamic properties of Ni(II) adsorption on $\text{NH}_2\text{-SBA-15}$

Temperature (K)	ΔH° (kJ mol^{-1})	ΔS° ($\text{kJ mol}^{-1} \text{K}^{-1}$)	ΔG° (kJ mol^{-1})
333			-34.33
313	93.8734	0.38812	-29.509
293			-19.098

Table 5
Adsorption capacities of nickel by various adsorbents

No.	Adsorbents	Adsorption capacity Q_{\max} mg g ⁻¹	References
1	Granular activated carbon (GAC)	8	[45]
2	Activated carbon from Lotus stalk	31.45	[46]
3	Activated carbon (Carbon-1)	28.25	[47]
4	Activated carbon (Carbon-2)	69.49	[47]
5	Functionalized SBA-15	90.1	This study

adsorption capacity of Ni(II) from other adsorbents materials. Functionalized mesoporous silica matrixes have been utilized to remove Ni(II) heavy metal ions from aqueous solutions because of their high surface area, large pore volume, plenty of well-distributed active sites and ease of diffusion for large reacting molecules through their nano channels.

4. Conclusions

This study shows that amine group grafted mesoporous silica (NH₂-SBA-15) can be used as an efficient adsorbent for Ni(II) heavy metal ion removal from aqueous solution. The removal efficiency of Ni(II) increased with an increase in pH (up to 5), time of contact, NH₂-SBA-15 dose and temperature. An increase in Ni(II) concentration, on the other hand, resulted in reducing Ni(II) removal efficiency. The temperature has a noticeable effect on Ni(II) removal. The latter has increased as the temperature increases from 293 to 333 K. The equilibrium data of Ni(II) adsorption at three different temperatures were well fitted by Langmuir isotherm model ($R^2 = 0.99$) which confirms the formation of monolayer Ni(II) coverage on the homogenous NH₂-SBA-15 surface. The kinetic adsorption data were well fitted by Pseudo-second-order kinetic model ($R^2 = 0.99$), and a general predictive model was obtained which describes the relationships between the adsorption uptake q (mg g⁻¹) along with solution temperature (K) and initial concentration (mg L⁻¹) at any time. The intraparticle adsorption kinetic model predicted that intraparticle diffusion is not the only rate that controlled the adsorption process. The thermodynamic parameters (ΔH° , ΔS° , and ΔG°) indicate that the whole adsorption process is of endothermic and spontaneous nature with a little degree of disorder in the adsorption system.

Acknowledgments

We gratefully acknowledge financial support from the Department of Chemical Engineering, University of Technology/Baghdad, Iraq.

References

- [1] F. Wang, X.W. Lu, X.-Y. Li, Selective removals of heavy metals (Pb²⁺, Cu²⁺, and Cd²⁺) from wastewater by gelation with alginate for effective metal recovery, *J. Hazard. Mater.*, 308 (2016) 75–83.
- [2] S. Babel, T.A. Kurniawan, Low-cost adsorbents for heavy metals uptake from contaminated water: a review, *J. Hazard. Mater.*, 97 (2013) 219–243.
- [3] T.M. Albayati, A.M. Doyle, Purification of aniline and nitro-substituted aniline contaminants from aqueous solution using beta zeolite, *Chem. Bulg. J. Sci. Educ.*, 23 (2014) 105–114.
- [4] S.S. Ahluwalia, D. Goyal, Microbial and plant derived biomass for removal of heavy metals from wastewater, *Bioresour. Technol.*, 98 (2007) 2243–2257.
- [5] T.M. Albayati, A.A. Sabri, D.B. Abed, Adsorption of binary and multi heavy metals ions from aqueous solution by amine functionalized SBA-15 mesoporous adsorbent in a batch system, *Desal. Wat. Treat.*, 151 (2019) 315–321.
- [6] M. Mareto, F. Bianchi, R. Vignola, S. Canepari, M. Baric, R. Iazzoni, M. Tagliabue, M.P. Papini, Microporous and mesoporous materials for the treatment of wastewater produced by petrochemical activities, *J. Cleaner Prod.*, 77 (2014) 22–34.
- [7] F.V. Pereira, L.V. Gurgel, S.F. de Aquino, L.F. Gil, Removal of Zn²⁺ from electroplating wastewater using modified wood sawdust and sugarcane bagasse, *J. Environ. Eng.*, 135 (2009) 341–350.
- [8] Mu. Naushad, T. Ahamad, G. Sharma, A.H. Al-Muhtaseb, A.B. Albadarin, M.A. Alam, Z.A. AlOthman, S.M. Alshehri, A.A. Ghfar, Synthesis and characterization of a new starch/SnO₂ nanocomposite for efficient adsorption of toxic Hg²⁺ metal ion, *Chem. Eng. J.*, 300 (2016) 306–316.
- [9] Mu. Naushad, T. Ahamad, B.M. Al-Maswari, A.A. Alqadami, S.M. Alshehri, Nickel ferrite bearing nitrogen-doped mesoporous carbon as efficient adsorbent for the removal of highly toxic metal ion from aqueous medium, *Chem. Eng. J.*, 330 (2017) 1351–1360.
- [10] H.N. Bhatti, J. Hayat, M. Iqbal, S. Noreen, S. Nawaz, Biocomposite application for the phosphate ions removal in aqueous medium, *J. Mater. Res. Technol.*, 7 (2018) 300–330.
- [11] A. Kausar, G. MacKinnon, A. Alharthi, J. Hargreaves, H.N. Bhatti, M. Iqbal, A green approach for the removal of Sr(II) from aqueous media: kinetics, isotherms and thermodynamic studies, *J. Mol. Liq.*, 257 (2018) 164–172.
- [12] B. Samiey, C.H. Cheng, J. Wu, Organic-inorganic hybrid polymers as adsorbents for removal of heavy metal ions from solutions: a review, *Materials*, 7 (2014) 673–726.
- [13] T.M. Albayati, A.A.A. Jassam, Synthesis and characterization of mesoporous materials as a carrier and release of prednisolone in drug delivery system, *J. Drug Delivery Sci. Technol.*, 53 (2019) 101176.
- [14] G.Q. Lu, X.S. Zhao, Nanoporous Materials – An Overview, G.Q. Lu, X.S. Zhao, Eds., Nanoporous Materials Science and Engineering, Ser. Chem. Eng., Imperial College Press, 4, 2004.
- [15] T.M. Albayati, Application of nanoporous material MCM-41 in a membrane adsorption reactor (MAR) as a hybrid process for removal of methyl orange, *Desal. Wat. Treat.*, 151 (2019) 138–144.
- [16] D. Zhao, Q. Huo, J. Feng, B.F. Chmelka, G.D. Stucky, Nonionic triblock and star diblock copolymer and oligomeric surfactant syntheses of highly ordered, hydrothermally stable, mesoporous silica structures, *J. Am. Chem. Soc.*, 120 (1998) 6024–6036.
- [17] D. Zhang, J.H. Li, Ordered SBA-15 mesoporous silica with high amino-functionalization for adsorption of heavy metal ions, *Chin. Sci. Bull.*, 58 (2013) 879–883.

- [18] A.A. Sabri, T.M. Albayati, D.B. Abed, Removal of cobalt (Co(II)) from aqueous solution by amino functionalized SBA-15, *Eng. Technol. J.*, 36 (2018) 703–708.
- [19] T.M. Albayati, A.M. Doyle, SBA-15 supported bimetallic catalysts for enhancement isomers production during *n*-heptane decomposition, *Int. J. Chem. Reactor Eng.*, 12 (2014) 345–354.
- [20] T.M.N. Albayati, S.E. Wilkinson, A.A. Garforth, A.M. Doyle, Heterogeneous alkane reactions over nanoporous catalysts, *Transp. Porous Media*, 104 (2014) 315–333.
- [21] T.M. Albayati, A.M. Doyle, Encapsulated heterogeneous base catalysts onto SBA-15 nanoporous material as highly active catalysts in the transesterification of sunflower oil to biodiesel, *J. Nanopart. Res.*, 17 (2015) 109.
- [22] A.A. Sabri, T.M. Albayati, R.A. Alazawi, Synthesis of ordered mesoporous SBA-15 and its adsorption of methylene blue, *Korean J. Chem. Eng.*, 32 (2015) 1835–1841.
- [23] I. Langmuir, The constitution and fundamental properties of solids and liquids. Part I. Solids, *J. Am. Chem. Soc.*, 38 (1916) 2221–2295.
- [24] T.W. Weber, R.K. Chakravorti, Pore and solid diffusion models for fixed-bed adsorbents, *Am. Inst. Chem. Eng. J.*, 20 (1974) 228–238.
- [25] M. Chen, Y. Chen, G.W. Diao, Adsorption kinetics and thermodynamics of methylene blue onto *p*-tert-butyl-calix[4,6,8] arena-bonded silica gel, *J. Chem. Eng. Data*, 55 (2010) 5109–5116.
- [26] H. Freundlich, Over the adsorption in solution, *J. Phys. Chem.*, 57 (1960) 385–471.
- [27] M. Temkin, V. Pyzhev, Kinetics of ammonia synthesis on promoted iron catalyst, *Acta Phys. Chim. Sin. USSR*, 12 (1940) 327–356.
- [28] S. Lagergren, About the theory of so-called adsorption of soluble substances, *Kungliga Svenska Vetenskapsakademiens Handlingar*, 24 (1898) 1–39.
- [29] Y. Ho, G. McKay, Pseudo-second-order model for sorption processes, *Process Biochem.*, 34 (1999) 451–465.
- [30] W.J. Weber, J.C. Morris, Kinetics of adsorption on carbon from solution, *J. Sanitary Eng. Div., Am. Soc. Civ. Eng.*, 89 (1963) 31–59.
- [31] S. Svilović, D. Rušić, R. Stipišić, Modeling batch kinetics of copper ions sorption using synthetic zeolite NaX, *J. Hazard. Mater.*, 170 (2009) 941–947.
- [32] D. Kavitha, C. Namasivayam, Experimental and kinetic studies on methylene blue adsorption by coir pith carbon, *Bioresour. Technol.*, 98 (2007) 14–21.
- [33] S. Wongsakulphasatch, An overview of applying surfactants to modified-functionalized nanoporous materials for metal ions sequestration, *Eng. J.*, 17 (2013) 29–37.
- [34] B.H. Aregawi, A.A. Mengistie, Removal of Ni(II) from aqueous solution using leaf, bark and seed of moringa stenopetala adsorbents, *Bull. Chem. Soc. Ethiop.*, 7 (2013) 35–47.
- [35] R. Cheraghali, H. Tavakoli, H. Sepehrian, Preparation, characterization and lead sorption performance of alginate-SBA-15 composite as a novel adsorbent, *Sci. Iranica.*, 20 (2013) 1028–1034.
- [36] A. Shahbazi, H. Younesi, A. Badiei, Functionalized SBA-15 mesoporous silica by melamine-based dendrimer amines for adsorptive characteristics of Pb(II), Cu(II) and Cd(II) heavy metal ions in batch and fixed bed column, *Chem. Eng. J.*, 168 (2011) 505–518.
- [37] J. Aguado, J.M. Arsuaga, A. Arencibia, M. Lindo, V. Gascón, Aqueous heavy metals removal by adsorption on amine-functionalized mesoporous silica, *J. Hazard. Mater.*, 163 (2008) 213–21.
- [38] A.K. Meena, G.K. Mishra, P.K. Rai, C. Rajagopal, P.N. Nagar, Removal of heavy metal ions from aqueous solutions using carbon aerogel as an adsorbent, *J. Hazard. Mater.*, 122 (2005) 161–170.
- [39] W. Guan, J.M. Pan, H.X. Ou, X. Wang, X.H. Zou, W. Hu, C.X. Li, X.Y. Wu, Removal of strontium(II) ions by potassium tetratitanate whisker and sodium trititanate whisker from aqueous solution: equilibrium, kinetics and thermodynamics, *Chem. Eng. J.*, 167 (2011) 215–222.
- [40] A. Arumugam, V. Ponnusami, Modified SBA-15 synthesized using sugarcane leaf ash for nickel adsorption, *Indian J. Chem. Technol.*, 20 (2013) 101–105.
- [41] M. Mureseanu, A. Reiss, I. Stefanescu, E. David, V. Parvulescu, G. Renard, V. Hulea, Modified SBA-15 mesoporous silica for heavy metal ions remediation, *Chemosphere*, 73 (2008) 1499–1504.
- [42] V. Manu, H. Mody, H. Bajaj, R. Jasra, Adsorption of Cu²⁺ on amino functionalized silica gel with different loading, *Ind. Eng. Chem. Res.*, 48 (2009) 8954–8960.
- [43] M. Najafi, Y. Yousefi, A. Rafati, Synthesis, characterization and adsorption studies of several heavy metal ions on amino-functionalized silica nano hollow sphere and silica gel, *Sep. Purif. Technol.*, 85 (2012) 193–205.
- [44] R.C. Bansal, M. Goyal, *Activated Carbon Adsorption*, CRC Press, Taylor & Francis Group, Boca Raton, 2005.
- [45] V.R. Kinkhikar, Removal of nickel (II) from aqueous solutions by adsorption with granular activated carbon (GAC), *Res. J. Chem. Sci.*, 2 (2012) 6–11.
- [46] L. Hui, H. Yuan, Y. Sung, T. Yang, L. Li, Adsorption behavior of Ni(II) on lotus stalks derived active carbon by phosphoric acid activation, *Desalination*, 268 (2011) 12–19.
- [47] R.M. Shrestha, M. Varga, I. Varga, A.P. Yadav, B.P. Pokharel, R.R. Pradhananga, Removal of Ni(II) from aqueous solution by adsorption onto activated carbon prepared from *Lapsi (Choerospondias axillaris)* seed stone, *J. Inst. Eng.*, 9 (2013) 166–174.